JOURNAL OF COMPUTATIONAL PHYSICS 90, 371–395 (1990)

Inviscid Flux-Splitting Algorithms for Real Gases with Non-equilibrium Chemistry

JIAN-SHUN SHUEN

Sverdrup Technology, Inc.,
NASA Lewis Research Center, Cleveland, Ohio 44135

MENG-SING LIOU

NASA Lewis Reseach Center, Cleveland, Ohio 44135

AND

BRAM VAN LEER

University of Michigan, Ann Arbor, Michigan 48109 and
Institute for Computational Mechanics in Propulsion (ICOMP),
NASA Lewis Research Center, Cleveland, Ohio 44135

Received August 31, 1988; revised June 30, 1989

Several flux-splitting methods for the inviscid terms of the compressible-flow equations are derived for gases that are not in chemical equilibrium. Formulas are presented for the extension to chemical nonequilibrium of the Steger–Warming and Van Leer flux-vector splittings, and the Roe flux-difference splitting. The splittings are incorporated in a TVD algorithm and applied to one-dimensional shock-tube and nozzle flows of dissociating air, includung five species and 11 reaction steps for the chemistry. © 1990 Academic Press, Inc.

1. INTRODUCTION

In the past decade various flux-splitting methods, for example, those of Steger and Warming [1], Van Leer [2], and Roe [3], have been used to solve aerodynamic problems based on the Euler equations for an ideal gas. With the renewed interest in high-temperature and chemically reacting flows, these methods have recently been extended to real gases by several researchers [4–10].

Colella and Glaz [4] presented a numerical procedure for obtaining the flux from the exact solution of the Riemann problem for a real gas, that is, a gas with a non-ideal equation of state (EOS). Grossman and Walters [5] extended the formulas of Steger and Warming, Van Leer, and Roe, introducing some simplifying assumptions and approximations that later were shown to be unnecessary. Vinokur and collaborators [6–8] produced a sequence of papers on the extension of these

0021-9991/90 $3.00

formulas to real gases, in which both the analysis of the numerical problem and the formulas produced become more and more sophiscated; numerical examples, though, are scant. Glaister [9] presented an elegant extension of Roe's "approximate Riemann solver." Liou, Van Leer, and Shuen [10] presented different extensions of these splittings, backed by a careful analysis. Their numerical results for one-dimensional shock-tube and nozzle flows at present appear to represent the state of the art.

All of the above references deal with real gases that are in chemical and thermal equilibrium, so that a unique EOS can be assumed to exist. For flows with finite Damköhler number, defined as the ratio of flow-residence time to chemical-reaction time, effects of chemical non-equilibrium are important; thus finite-rate chemistry must enter the analysis.

Just as for gases in equilibrium, the literature on numerical flux function for non-equilibrium gases is rapidly expanding. Without claiming to be comprehensive, we list some very recent reports. Grossman and Cinnella [11] extended the equilibrium methods of [5] to incorporate both chemical and thermal (vibrational) non-equilibrium. Abgrall [12] formulated Roe's splitting for chemical non-equilibrium gases and performed numerical tests with a second-order, semi-implicit TVD scheme. Furthermore, Grossman *et al.* [13] contributed a survey of several methods suggested to date, including numerical comparisons of both equilibrium and non-equilibrium flux formulas.

In the present paper we extend the previously derived [10] real-gas version of the flux-splitting of Steger and Warming, Van Leer, and Roe, to gases that are not in chemical equilibrium. These splittings are incorporated in a second-order TVD scheme [14], by which solutions are obtained for the same shock-tube and nozzle flows as computed in [10] with equilibrium chemistry.

The layout of this paper is as follows. In Section 2 we discuss the equation of state and related thermodynamic quantities for gases in chemical non-equilibrium. The essence of the paper is in Section 3, where the detailed derivation of split-flux formulas is presented. In Section 4 we describe a chemical system for air dissociation and recombination. Finally, in Section 5 we describe further details of the numerical methods and show numerical results for one-dimensional shock-tube and nozzle flows of air in chemical non-equilibrium.

2. Equation of State

We begin by assuming that the macroscopic thermodynamic properties of a gas consisting of N species can be related through the general equation of state,

$$p = p(\rho, e, C_1, C_2, ..., C_{N-1}), \tag{2.1}$$

where p, ρ, e, C_i are, respectively, the pressure, density, specific internal energy, and mass concentration for species i. Note that $\sum_{i=1}^{N} C_i = \rho$; therefore, if the total mass

density ρ is regarded as an independent quantity, only $\mathbf{N}-1$ concentration are independent for a chemical system of $\mathbf{N}$ species. For chemical nonequilibrium flows, the values of C_i's depend not only on the transport of fluid, but also on the progress of chemical reactions; therefore, unlike for equilibrium gases [10], *a priori* determination of an EOS is not possible, and the EOS has to be constructed along with the solution process. If the inter-molecular forces and the volume occupeid by molecules are negligible, pressure p can be expressed as

$$p = R_u T \sum_{i=1}^{N} \frac{C_i}{W_i}, \tag{2.2}$$

where R_u is the universal gas constant, T the temperature, and W_i the molecular weight of species i.

The speed of sound is given by

$$a^2 \equiv \left(\frac{\partial p}{\partial \rho}\right)_s = p_\rho + p_e p/\rho^2 + \sum_{i=1}^{N-1} C_i p_{C_i}/\rho. \tag{2.3}$$

Here and throughout this paper, p_ρ, p_e, and p_{C_i} denote the partial derivatives of p with respect to ρ, e, and C_i with other variables held fixed. This speed is generally known as the "frozen speed of sound," because it does not take into account the possible variation of chemical composition in a sound wave (this can be included in an equilibrium model, leading to the so-called "equilibrium speed of sound"). To facilitate the evaluation of the pressure derivatives in Eq. (2.3), Eq. (2.2) is recast in the following form:

$$p = R_u T \left[\frac{\rho}{W_N} + \sum_{i=1}^{N-1} C_i \left(\frac{1}{W_i} - \frac{1}{W_N}\right)\right]. \tag{2.4}$$

The pressure derivatives are then given by

$$\begin{aligned} p_\rho = \left(\frac{\partial p}{\partial \rho}\right)_{e, C_i, i=1, N-1} &= \frac{R_u T}{W_n} + \frac{\rho R_u}{W}\left(\frac{\partial T}{\partial \rho}\right)_{e, C_i, i=1, N-1} \\ &= \frac{R_u T}{W_N} + \frac{R_u}{W C_v} \sum_{i=1}^{N-1} \frac{C_i}{\rho}(e_i - e_N), \end{aligned} \tag{2.5a}$$

$$\begin{aligned} p_e = \left(\frac{\partial p}{\partial e}\right)_{\rho, C_i, i=1, N-1} &= \frac{\rho R_u}{W}\left(\frac{\partial T}{\partial e}\right)_{\rho, C_i, i=1, N-1} \\ &= \frac{\rho R_u}{W C_v}, \end{aligned} \tag{2.5b}$$

and

$$p_{C_i} = \left(\frac{\partial p}{\partial C_i}\right)_{\rho, e, C_{j,j=1,N-1, j\neq i}} = R_u T\left(\frac{1}{W_i} - \frac{1}{W_N}\right) + \frac{\rho R_u}{W}\left(\frac{\partial T}{\partial C_i}\right)_{\rho, e, C_{j,j=1,N-1, j\neq i}}$$

$$= R_u T\left(\frac{1}{W_i} - \frac{1}{W_N}\right) - \frac{R_u}{WC_v}(e_i - e_N), \tag{2.5c}$$

where $W = ((1/\rho)\sum_{i=1}^{N}(C_i/W_i))^{-1}$ is the molecular weight of the gas mixture, $C_v = \sum_{i=1}^{N} C_i C_{p_i}/\rho - R_u/W$ is the constant-volume specific heat of the gas mixture, and $e_i = \int_{T_{\text{ref}}}^{T} C_{p_i}\, dT + h_{f_i}^0 - R_u T/W_i$, C_{p_i}, and $h_{f_i}^0$, are the specific internal energy, the constant-pressure specific heat, and the heat of formation, respectively, of the ith species; T_{ref} is the reference temperature for thermodynamic properties.

To close the system, we still need to determine the temperature. Here the temperature T is calculated after the flow properties ρ, e, and C_i are obtained, using the equation

$$\rho e = \sum_{i=1}^{N} C_i\left(\int_{T_{\text{ref}}}^{T} C_{p_i}\, dT + h_{f_i}^0\right) - p. \tag{2.6}$$

The specific heat of individual species C_{p_i} appearing in the above formulation is calculated by methods of statistical mechanics and is fitted by a fourth-order polynomial of temperature [15]. The C_{p_i} polynomials so generated in this study are valid for the temperature range of 200 to 15,000 K.

It is interesting to note that upon substitution of the pressure derivatives in Eq. (2.3) by means of Eqs. (2.4)–(2.5c), the expression for the frozen speed of sound simplifies to

$$a^2 = \frac{p}{\rho}\left(1 + \frac{R}{C_v}\right), \tag{2.7}$$

where $R = R_u \sum_{i=1}^{N} C_i/\rho W_i$ is the gas constant for the mixture. This simple relationship, as pointed out by B. Stoufflet [16], may be obtained directly from the ideal gas law, i.e., $p = \rho RT$, assuming a thermally perfect gas with a frozen chemical composition.

3. Construction of Split Fluxes

The derivations presented in this section closely follow the methodology of our previous work for equilibrium gases [10]. The appearance of mass fluxes for the different species, however, introduces additional complexity.

We shall restrict ourselves to the splitting of fluxes for one-dimensional flow and therefore consider the 1D Euler equations,

$$\frac{\partial \mathbf{U}}{\partial t} + \frac{\partial F(\mathbf{U})}{\partial x} = \mathbf{S}, \tag{3.1}$$

where

$$\mathbf{U}=\begin{pmatrix}\rho\\ \rho u\\ \rho E\\ C_1\\ C_2\\ \vdots\\ C_{N-1}\end{pmatrix},\qquad \mathbf{F}=\begin{pmatrix}\rho u\\ \rho u^2+p\\ u(\rho E+p)\\ uC_1\\ uC_2\\ \vdots\\ uC_{N-1}\end{pmatrix},\qquad \mathbf{S}=\begin{pmatrix}0\\ 0\\ 0\\ S_1\\ S_2\\ \vdots\\ S_{N-1}\end{pmatrix},$$

with $E=e+\frac{1}{2}u^2$, and S_i is the source term for species i due to chemical reactions.

If the EOS is expressed in terms of the flow variables, viz. as $p=p(\rho(\mathbf{U}), e(\mathbf{U}), C_1(\mathbf{U}), C_2(\mathbf{U}), \ldots, C_{N-1}(\mathbf{U}))$, the pressure derivatives with respect to flow variables $\mathbf{U}$ can be readily derived. By the chain rule for partial derivatives we have

$$\left.\frac{\partial p}{\partial \rho}\right|_{\rho u,\rho_E,C_{i,i=1,N-1}}=\left.\frac{\partial p}{\partial \rho}\right|_{e,C_{i,i=1,N-1}}+\left.\frac{\partial p}{\partial e}\right|_{\rho,C_{i,i=1,N-1}}\left.\frac{\partial e}{\partial \rho}\right|_{\rho u,\rho_E,C_{i,i=1,N-1}}$$

$$=p_\rho+\frac{p_e}{\rho}\left(-H+\frac{p}{\rho}+u^2\right), \tag{3.2a}$$

$$\left.\frac{\partial p}{\partial(\rho u)}\right|_{\rho,\rho_E,C_{i,i=1,N-1}}=\left.\frac{\partial p}{\partial e}\right|_{\rho,C_{i,i=1,N-1}}\left.\frac{\partial e}{\partial(\rho u)}\right|_{\rho,\rho_E,C_{i,i=1,N-1}}$$

$$=\frac{-up_e}{\rho}, \tag{3.2b}$$

$$\left.\frac{\partial p}{\partial(\rho E)}\right|_{\rho,\rho u,C_{i,i=1,N-1}}=\left.\frac{\partial p}{\partial e}\right|_{\rho,C_{i,i=1,N-1}}\left.\frac{\partial e}{\partial(\rho E)}\right|_{\rho,\rho u,C_{i,i=1,N-1}}$$

$$=\frac{pe}{\rho}, \tag{3.2c}$$

and

$$\left.\frac{\partial p}{\partial C_i}\right|_{\rho,\rho u,\rho E,C_{j,j=1,N-1,j\neq i}}=\left.\frac{\partial p}{\partial e}\right|_{\rho,C_{i,i=1,N-1}}\left.\frac{\partial e}{\partial C_i}\right|_{\rho,\rho u,\rho E,C_{j,j=1,N-1,j\neq i}}$$

$$+\left.\frac{\partial p}{\partial C_i}\right|_{\rho,e,C_{j,j=1,N-1,j\neq i}}$$

$$=p_{C_i}, \tag{3.2d}$$

where $H=h+\frac{1}{2}u^2=e+\frac{1}{2}u^2+(p/\rho)=E+(p/\rho)$.

These derivatives are used in evaluating the Jacobian matrix of the flux vector,

which is needed for several split-flux algorithms. The Jacobian matrix can be written as

$$\mathbf{A} = \frac{\partial \mathbf{F}}{\partial \mathbf{U}} = \mathbf{A}_e + \mathbf{A}_\rho, \tag{3.3a}$$

where

$$\mathbf{A}_e = \begin{bmatrix} 0 & 1 & 0 & 0 & 0 & 0 & 0 \\ -u^2\left(1-\frac{p_e}{2\rho}\right)+\frac{(p-p_e e)}{\rho} - \sum_{i=1}^{N-1}\frac{C_i}{\rho}p_{C_i} & \left(2u-u\frac{p_e}{\rho}\right) & \frac{p_e}{\rho} & p_{C_1} & p_{C_2} & p_{C_3} & p_{C_4} \\ u\left[-H+u^2\frac{p_e}{2\rho}+\frac{(p-p_e e)}{\rho} - \sum_{i=1}^{N-1}\frac{C_i}{\rho}p_{C_i}\right] & \left(H-u^2\frac{p_e}{\rho}\right) & u\left(1+\frac{p_e}{\rho}\right) & up_{C_1} & up_{C_2} & up_{C_3} & up_{C_4} \\ -u\frac{C_1}{\rho} & \frac{C_1}{\rho} & 0 & u & 0 & 0 & 0 \\ -u\frac{C_2}{\rho} & \frac{C_2}{\rho} & 0 & 0 & u & 0 & 0 \\ -u\frac{C_3}{\rho} & \frac{C_3}{\rho} & 0 & 0 & 0 & u & 0 \\ -u\frac{C_4}{\rho} & \frac{C_4}{\rho} & 0 & 0 & 0 & 0 & u \end{bmatrix} \tag{3.3b}$$

contains the derivative p_e, and the matrix containing p_ρ is

$$\mathbf{A}_\rho = \begin{bmatrix} 0 & 0 & 0 & 0 & 0 & 0 & 0 \\ p_\rho - \frac{p}{\rho} + \sum_{i=1}^{N-1}\frac{C_i}{\rho}p_{C_i} & 0 & 0 & 0 & 0 & 0 & 0 \\ u\left(p_\rho - \frac{p}{\rho} + \sum_{i=1}^{N-1}\frac{C_i}{\rho}p_{C_i}\right) & 0 & 0 & 0 & 0 & 0 & 0 \\ 0 & 0 & 0 & 0 & 0 & 0 & 0 \\ 0 & 0 & 0 & 0 & 0 & 0 & 0 \\ 0 & 0 & 0 & 0 & 0 & 0 & 0 \\ 0 & 0 & 0 & 0 & 0 & 0 & 0 \end{bmatrix}. \tag{3.3c}$$

For clarity of presentation, in the above derivation and the rest of of the paper we have set $\mathbf{N} = 5$, which is the number of species considered in our chemistry model (see Section 4).

The eigenvalues of these matrices are, respectively:

$$\lambda(\mathbf{A}) = u - a,\ u,\ u + a,\ u,\ u,\ u,\ u, \tag{3.4a}$$

$$\lambda(\mathbf{A}_e) = u - a_e,\ u,\ u + a_e,\ u,\ u,\ u,\ u, \tag{3.4b}$$

$$\lambda(\mathbf{A}_\rho) = 0,\ 0,\ 0,\ 0,\ 0,\ 0,\ 0, \tag{3.4c}$$

where $a_e^2 = p/\rho + pp_e/\rho^2 = a^2 - (p_\rho - p/\rho + \sum_{i=1}^{N-1} (C_i/\rho)\, p_{C_i})$. Thus the matrices $\mathbf{A}$ and $\mathbf{A}_e$ have a complete set of eigenvectors, and $\mathbf{A}_\rho$ does not. It can be shown that $a_e = a$ and $\mathbf{A}_e = \mathbf{A}$ for a gas in which p has the form $p = \rho f(T)$, i.e., a thermally perfect gas.

For real gases one finds that the inviscid flux vector $\mathbf{F}$ no longer possesses the property of homogeneity, but rather is a sum of a homogeneous and an inhomogeneous part:

$$\mathbf{F} = \mathbf{F}_h + \mathbf{F}_{in}; \tag{3.5}$$

here $\mathbf{F}_h = \mathbf{AU}$ and $\mathbf{F} = \mathbf{A}_e\mathbf{U}$, yielding $\mathbf{F}_{in} = -\mathbf{A}_\rho\mathbf{U}$.

Since the matrix $\mathbf{A}$ has a complete set of eigenvectors, it can be diagonalized by a similarity matrix $\mathbf{S}$ whose column vectors are the right eigenvectors of $\mathbf{A}$:

$$\mathbf{A} = \mathbf{S}\Lambda\mathbf{S}^{-1}, \qquad \operatorname{diag}\Lambda = \lambda(\mathbf{A}). \tag{3.6a}$$

The matrix $\mathbf{S}$ and its inverse $\mathbf{S}^{-1}$ are frequently used in numerical flux functions and are given below for completeness:

$$\mathbf{S} = \begin{bmatrix} 1 & \frac{\rho}{\sqrt{2}\,a} & \frac{\rho}{\sqrt{2}\,a} & 0 & 0 & 0 & 0 \\ u & \frac{\rho(u+a)}{\sqrt{2}\,a} & \frac{\rho(u-a)}{\sqrt{2}\,a} & 0 & 0 & 0 & 0 \\ H - \frac{\rho a^2}{p_e} & \frac{\rho}{\sqrt{2}\,a}(H+ua) & \frac{\rho}{\sqrt{2}\,a}(H-ua) & \frac{-\rho^2 p_{C_1}}{p_e} & \frac{-\rho^2 p_{C_2}}{p_e} & \frac{-\rho^2 p_{C_3}}{p_e} & \frac{-\rho^2 p_{C_4}}{p_e} \\ \frac{C_1}{\rho} & \frac{C_1}{\sqrt{2}\,a} & \frac{C_1}{\sqrt{2}\,a} & \rho & 0 & 0 & 0 \\ \frac{C_2}{\rho} & \frac{C_2}{\sqrt{2}\,a} & \frac{C_2}{\sqrt{2}\,a} & 0 & \rho & 0 & 0 \\ \frac{C_3}{\rho} & \frac{C_3}{\sqrt{2}\,a} & \frac{C_3}{\sqrt{2}\,a} & 0 & 0 & \rho & 0 \\ \frac{C_4}{\rho} & \frac{C_4}{\sqrt{2}\,a} & \frac{C_4}{\sqrt{2}\,a} & 0 & 0 & 0 & \rho \end{bmatrix}, \tag{3.6b}$$

and

$$\mathbf{S}^{-1}=\begin{pmatrix}
1-\frac{1}{a^2}\left[\left(p_\rho+\frac{pp_e}{\rho^2}\right)-\frac{p_e}{\rho}(H-u^2)\right] & \frac{up_e}{\rho a^2} & -\frac{p_e}{\rho a^2} & -\frac{p_{C_1}}{a^2} & -\frac{p_{C_2}}{a^2} & -\frac{p_{C_3}}{a^2} & -\frac{p_{C_4}}{a^2} \\
\frac{1}{\sqrt{2}\,\rho a}\left[-ua+\left(p_\rho+\frac{pp_e}{\rho^2}\right)-\frac{p_e}{\rho}(H-u^2)\right] & \frac{1}{\sqrt{2}\,\rho a}\left(a-\frac{up_e}{\rho}\right) & \frac{1}{\sqrt{2}\,\rho a}\frac{p_e}{\rho} & \frac{p_{C_1}}{\sqrt{2}\,\rho a} & \frac{p_{C_2}}{\sqrt{2}\,\rho a} & \frac{p_{C_3}}{\sqrt{2}\,\rho a} & \frac{p_{C_4}}{\sqrt{2}\,\rho a} \\
\frac{1}{\sqrt{2}\,\rho a}\left[ua+\left(p_\rho+\frac{pp_e}{\rho^2}\right)-\frac{p_e}{\rho}(H-u^2)\right] & -\frac{1}{\sqrt{2}\,\rho a}\left(a+\frac{up_e}{\rho}\right) & \frac{1}{\sqrt{2}\,\rho a}\frac{p_e}{\rho} & \frac{p_{C_1}}{\sqrt{2}\,\rho a} & \frac{p_{C_2}}{\sqrt{2}\,\rho a} & \frac{p_{C_3}}{\sqrt{2}\,\rho a} & \frac{p_{C_4}}{\sqrt{2}\,\rho a} \\
-\frac{C_1}{\rho^2} & 0 & 0 & \frac{1}{\rho} & 0 & 0 & 0 \\
-\frac{C_2}{\rho^2} & 0 & 0 & 0 & \frac{1}{\rho} & 0 & 0 \\
-\frac{C_3}{\rho^2} & 0 & 0 & 0 & 0 & \frac{1}{\rho} & 0 \\
-\frac{C_4}{\rho^2} & 0 & 0 & 0 & 0 & 0 & \frac{1}{\rho}
\end{pmatrix}. \tag{3.6c}$$

3.1. *Steger–Warming Splitting*

By splitting the eigenvalues of $\mathbf{A}$ according to their signs, i.e.,

$$\Lambda=\Lambda^+ + \Lambda^-, \tag{3.7}$$

the chemical nonequilibrium version of Steger–Warming flux-vector splitting is obtained by writing $\mathbf{F}_h=\mathbf{F}_h^+ + \mathbf{F}_h^- = \mathbf{A}^+\mathbf{U}+\mathbf{A}^-\mathbf{U}$, with $\mathbf{A}^\pm = \mathbf{S}\Lambda^\pm\mathbf{S}^{-1}$. Specifically, define

$$\begin{aligned}
\lambda_1^\pm &= (u \pm |u|)/2, \\
\lambda_2^\pm &= (u+a \pm |u+a|)/2, \\
\lambda_3^\pm &= (u-a \pm |u-a|)/2,
\end{aligned} \tag{3.8}$$

then components of $\mathbf{F}_h^\pm = (\mathbf{F}_{h1}^\pm, \mathbf{F}_{h2}^\pm, \ldots, \mathbf{F}_{h7}^\pm)'$ are

$$\mathbf{F}_{h1}^{\pm}=\frac{1}{a^2}\left[\lambda_1^{\pm}\frac{pp_e}{\rho}+\frac{\lambda_2^{\pm}}{2}\left(\rho a^2-\frac{pp_e}{\rho}\right)+\frac{\lambda_3^{\pm}}{2}\left(\rho a^2-\frac{pp_e}{\rho}\right)\right], \tag{3.9a}$$

$$\mathbf{F}_{h2}^{\pm}=\frac{1}{a^2}\left[\lambda_1^{\pm}\frac{upp_e}{\rho}+\lambda_2^{\pm}\frac{(u+a)}{2}\left(\rho a^2-\frac{pp_e}{\rho}\right)+\lambda_3^{\pm}\frac{(u-a)}{2}\left(\rho a^2-\frac{pp_e}{\rho}\right)\right], \tag{3.9b}$$

$$\mathbf{F}_{h3}^{\pm}=\frac{1}{a^2}\left[\lambda_1^{\pm}\left(\frac{pp_e}{\rho}H-pa^2\right)+\lambda_2^{\pm}\frac{(H+ua)}{2}\left(\rho a^2-\frac{pp_e}{\rho}\right)+\lambda_3^{\pm}\frac{(H-ua)}{2}\left(\rho a^2-\frac{pp_e}{\rho}\right)\right], \tag{3.9c}$$

$$\mathbf{F}_{h4}^{\pm}=\frac{C_1}{\rho}\mathbf{F}_{h1}^{\pm}, \tag{3.9d}$$

$$\mathbf{F}_{h5}^{\pm}=\frac{C_2}{\rho}\mathbf{F}_{h1}^{\pm}, \tag{3.9e}$$

$$\mathbf{F}_{h6}^{\pm}=\frac{C_3}{\rho}\mathbf{F}_{h1}^{\pm}, \tag{3.9f}$$

$$\mathbf{F}_{h7}^{\pm}=\frac{C_4}{\rho}\mathbf{F}_{h1}^{\pm}. \tag{3.9a}$$

These split fluxes are suited for upwind differencing. It should be pointed out that the true frozen speed of sound a is used in the splitting. Since $\mathbf{A}_\rho$ does not have a complete set of eigenvectors, a system of equations that consists of $\mathbf{F}_{\text{in}}$ alone does not have a hyperbolic character. In consequence, central differencing for the inhomogeneous flux $\mathbf{F}_{\text{in}}$ may be appropriate. Hence, just as in [10] for the equilibrium case, the split flux $\mathbf{F}$ can be expressed as

$$\mathbf{F}^{\pm}=\mathbf{F}_h^{\pm}+\tfrac{1}{2}\mathbf{F}_{\text{in}}. \tag{3.10}$$

The numerical tests of Section 5 confirm that this leads to a stable method.

3.2. *Van Leer Splitting*

In our previous study [10], we have extended the Van Leer splitting to a general equilibrium gas. The derivation in [10], which includes a family of flux choices, is independent of the EOS used and does not require homogeneity of the flux vector. The further generalization of Van Leer splitting to a gas not in chemical equilibrium is straightforward; the formulas are given below.

The splitting has the standard form

$$\mathbf{F}=\mathbf{F}^{+}+\mathbf{F}^{-}, \tag{3.11}$$

and is carried out only when the eigenvalues have mixed signs, i.e., as $M^2<1$ for

the system (3.1) with eigenvalues (3.4a); M is the local Mach number. The split fluxes of mass, momentum, and energy fluxes are

$$\mathbf{F}_1^{\pm} = \pm\tfrac{1}{4}\rho a(M \pm 1)^2, \tag{3.12a}$$

$$\mathbf{F}_2^{\pm} = \mathbf{F}_1^{\pm}\left[u - \frac{p}{\rho a^2}(u \mp 2a)\right], \tag{3.12b}$$

$$\mathbf{F}_3^{\pm} = \mathbf{F}_1^{\pm}[H - m(u \mp a)^2].$$

Exactly as in the equilibrium case [10], the parameter m generates a family of splittings; Van Leer splitting is a member of this family, found by requiring that the terms in the square bracket of the $\mathbf{F}_3^{\pm}$ fluxes form a perfect square. This leads to

$$m = \frac{h/a^2}{1 + 2h/a^2}$$

and

$$\mathbf{F}_3^{\pm} = \frac{1}{2}\mathbf{F}_1^{\pm}\frac{(ua \pm 2h)^2}{(a^2 + 2h)}. \tag{3.12c}$$

The concentration fluxes simply follow from a linear convection principle, i.e.,

$$\mathbf{F}_4^{\pm} = \frac{C_1}{\rho}\mathbf{F}_1^{\pm}, \tag{3.12d}$$

$$\mathbf{F}_5^{\pm} = \frac{C_2}{\rho}\mathbf{F}_1^{\pm}, \tag{3.12e}$$

$$\mathbf{F}_6^{\pm} = \frac{C_3}{\rho}\mathbf{F}_1^{\pm}, \tag{3.12f}$$

$$\mathbf{F}_7^{\pm} = \frac{C_4}{\rho}\mathbf{F}_1^{\pm}. \tag{3.12g}$$

3.3. *Roe Splitting*

To construct Roe's flux-difference splitting, one defines an average state $\hat{\mathbf{U}}$ such that

$$\Delta\mathbf{F} = \hat{\mathbf{A}}\Delta\mathbf{U}, \tag{3.13a}$$

$$\hat{\mathbf{A}} = \hat{\mathbf{A}}(\hat{U}), \tag{3.13b}$$

$$\hat{\mathbf{U}} = \hat{\mathbf{U}}(\mathbf{U}_L, \mathbf{U}_R), \tag{3.13c}$$

where

$$\Delta(\cdot) = (\cdot)_R - (\cdot)_L,$$

and

$$\mathbf{A}(\mathbf{U}) = \frac{\partial \mathbf{F}}{\partial \mathbf{U}}$$

$$= \begin{bmatrix} 0 & 1 & 0 & 0 & 0 & 0 & 0 \\ -u^2\left(1-\frac{\cdot}{2\rho}\right)+p_\rho-\frac{p_e e}{\rho} & \left(2u-u\frac{p_e}{\rho}\right) & \frac{p_e}{\rho} & p_{C_1} & p_{C_2} & p_{C_3} & p_{C_4} \\ u\left(-H+u^2\frac{p_e}{2\rho}+p_\rho-\frac{p_e e}{\rho}\right) & \left(H-u^2\frac{p_e}{\rho}\right) & u\left(1+\frac{p_e}{\rho}\right) & up_{C_1} & up_{C_2} & up_{C_3} & up_{C_4} \\ -u\frac{C_1}{\rho} & \frac{C_1}{\rho} & 0 & u & 0 & 0 & 0 \\ -u\frac{C_2}{\rho} & \frac{C_2}{\rho} & 0 & 0 & u & 0 & 0 \\ -u\frac{C_3}{\rho} & \frac{C_3}{\rho} & 0 & 0 & 0 & u & 0 \\ -u\frac{C_4}{\rho} & \frac{C_4}{\rho} & 0 & 0 & 0 & 0 & u \end{bmatrix} \tag{3.14}$$

is the matrix defined in (3.3a).

In the case of an ideal, non-reacting gas, the average state $\hat{\mathbf{U}}$ is easily found, since (3.13a) represents three simple equations with three unknowns. Such a state was derived by Roe [3]. For a real gas, this simplicity is lost. For 1D flow of a chemical system of $\mathbf{N}$ species, (3.13a) consists of $\mathbf{N}+2$ equations. By a careful examination of (3.14) we find that, for $\mathbf{N}=5$, there are fourteen (rather than seven) independent quantities (state variables and their derivatives) needed in computing $\mathbf{A}(\mathbf{U})$. In order to find a practical formula for $\hat{\mathbf{A}}$ we must relax the constraint (3.13b) and allow independent averages of these 14 state quantities to enter the elements of $\hat{\mathbf{A}}$; we shall choose the set $(\hat{u}, \hat{\rho}, \hat{e}, \hat{H}, \hat{C}_{i,i=1,4}, \hat{p}_\rho, \hat{p}_e, \hat{p}_{C_{i,i=1,4}})$. We emphasize that, although $p_\rho = p_\rho(\rho, e, C_{i,i=1,N-1})$, $\hat{p}_\rho$ is not obtained by substituting $(\hat{\rho}, \hat{e}, \hat{C}_{i,i=1,N-1})$ into (2.5a), but must be defined separately; this is also the case for $\hat{p}_e$ and $\hat{p}_{C_i}$.

Let the Roe-average operator μ be defined as usual:

$$\mu(f) = \frac{r_{\mathrm{R}} f_{\mathrm{R}} + r_{\mathrm{L}} f_{\mathrm{L}}}{r_{\mathrm{R}} + r_{\mathrm{L}}}, \qquad r = \rho^{1/2}; \tag{3.15}$$

as in the equilibrium case [10] we find

$$\hat{\rho} = r_{\mathrm{L}} r_{\mathrm{R}}, \tag{3.16a}$$

$$\hat{u} = \mu(u), \tag{3.16b}$$

$$\hat{e} = \mu(e), \tag{3.16c}$$

$$\hat{H} = \mu(H), \tag{3.16d}$$

while the species mass fractins C_i/ρ are averaged similarly:

$$\widehat{\left(\frac{C_i}{\rho}\right)} = \mu\left(\frac{C_i}{\rho}\right), \qquad i = 1, ..., N_1. \tag{3.16e}$$

Left to be satisfied is the condition

$$\Delta p = \hat{p}_\rho \Delta\rho + \hat{p}_e \Delta e + \sum_{i=1}^{N-1} \hat{p}_{C_i} \Delta C_i, \tag{3.17}$$

which means we have to define the averages of the pressure derivatives, $\hat{p}_\rho$, $\hat{p}_e$, and $\hat{p}_{C_i}$, $i = 1, ..., N-1$. For a gas in chemical nonequilibrium, (3.17) provides only one relation for the variables $\hat{p}_\rho$, $\hat{p}_e$, and $\hat{p}_{C_i}$, $i = 1, ..., N-1$; thus the definitions for the averages of these pressure derivatives are not unique. The formulas we propose below reduce to those derived in [10] for a gas in chemical equilibrium.

As in [10], we shall derived values of $\hat{p}_\rho$, $\hat{p}_e$, and $\hat{p}_{C_i}$, $i = 1, ..., N-1$, that are as close as possible to the *consistent* derivative values, i.e., the values computed at the average state $(\hat{\rho}, \hat{e}, \hat{C}_1, \hat{C}_2, ..., \hat{C}_{N-1})$. We therefore introduce

$$\begin{aligned} \bar{p}_\rho &= p_\rho(\hat{\rho}, \hat{e}, \hat{C}_1, ..., \hat{C}_{N-1}), \\ \bar{p}_e &= p_e(\hat{\rho}, \hat{e}, \hat{C}_1, ..., \hat{C}_{N-1}), \\ \bar{p}_{C_i} &= p_{C_i}(\hat{\rho}, \hat{e}, \hat{C}_1, ..., \hat{C}_{N-1}), \qquad i = 1, ..., N-1, \end{aligned} \tag{3.18}$$

Next, we need a density unit R, energy unit E, and concentration units M_i's so that the derivatives are scaled properly. Equation (3.17) may be written as

$$\left(\frac{\Delta e}{\Delta p} R\right)\frac{\hat{p}_e}{R} + \left(\frac{\Delta\rho}{\Delta p} E\right)\frac{\hat{p}_\rho}{E} + \sum_{i=1}^{N-1}\left(\frac{\Delta C_i}{\Delta p} M_i\right)\frac{\hat{p}_{C_i}}{M_i} = 1, \tag{3.19a}$$

or, simply

$$\alpha x + \beta y + \sum_{i=1}^{N-1} \gamma_i z_i = 1, \tag{3.19b}$$

with

$$\begin{aligned} &\alpha \equiv \frac{\Delta e}{\Delta p} R, \qquad \beta \equiv \frac{\Delta\rho}{\Delta p} E, \qquad \gamma_i \equiv \frac{\Delta C_i}{\Delta p} M_i, \\ &x \equiv \frac{\hat{p}_e}{R}, \qquad y \equiv \frac{\hat{p}_\rho}{E}, \qquad z_i \equiv \frac{\hat{p}_{C_i}}{M_i}. \end{aligned} \tag{3.19c}$$

The set of values $(x_0, y_0, z_{1_0}, z_{2_0}, ..., z_{(N-1)_0}) \equiv (\bar{p}_e/R, \bar{p}_\rho/E, \bar{p}_{C_1}/M_1, \bar{p}_{C_2}/M_2, ..., \bar{p}_{C_{N-1}}/M_{N-1})$ in general do not satisfy Eq. (3.19a), i.e., the point $Q \equiv (x_0, y_0, z_{1_0}, z_{2_0}, ..., z_{(N-1)_0})$ in the $(x, y, z_1, z_2, ..., z_{N-1})$ plane does not lie on the surface D represented by Eq. (3.19b); see the sketch.

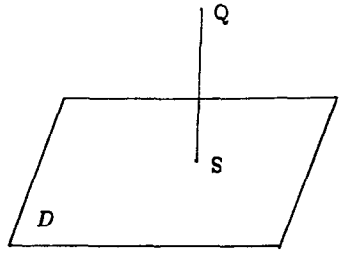

The point on D closest to Q is the projection S of Q onto D; this is the optimal choice regarding consistency of $(\hat{p}_e, \hat{p}_\rho, \hat{p}_{C_i, i=1,N-1})$ with $(\bar{p}_e, \bar{p}_\rho, \bar{p}_{C_i, i=1,N-1})$ and other independently defined average state variables, for the given distance scaling $(R, E, M_{i, i=1,N-1})$. The coordinates of **S** are formed by combining Eq. (3.19b) with the equations for **SQ**:

$$\begin{aligned} &\alpha x_s + \beta y_s + \sum_{i=1}^{N-1} \gamma_i z_{i_s} = 1, \\ &\beta(x_s - x_0) - \alpha(y_s - y_0) = 0, \\ &\gamma_i(x_s - x_0) - \alpha(z_{i_s} - z_{i_0}) = 0, \qquad i = 1, ..., N-1, \end{aligned} \tag{3.20}$$

yielding

$$\begin{aligned} x_s &= x_0 + \alpha\Omega, \\ y_s &= y_0 + \beta\Omega, \\ z_{i_s} &= z_{i_0} + \gamma_i\Omega, \qquad i = 1, ..., N-1, \end{aligned} \tag{3.21}$$

where

$$\Omega = \frac{1 - \alpha x_0 - \beta y_0 - \gamma_1 z_{1_0} - \cdots - \gamma_{N-1} z_{(N-1)_0}}{\alpha^2 + \beta^2 + \gamma_1^2 + \cdots + \gamma_{N-1}^2}.$$

An obvious scaling is

$$R = \frac{\Delta p}{\Delta e}, \qquad E = \frac{\Delta p}{\Delta \rho}, \qquad M_i = \frac{\Delta p}{\Delta C_i}, \qquad i = 1, ..., N-1, \tag{3.22a}$$

yielding $\alpha - \beta = \gamma_i = 1$; this leads to

$$\hat{p}_e = \bar{p}_e + \frac{1}{N+1}\,\delta p/\Delta e,$$

$$\hat{p}_\rho = \bar{p}_\rho + \frac{1}{N+1}\,\delta p/\Delta \rho, \tag{3.22b}$$

$$\hat{p}_{C_i} = \bar{p}_{C_i} + \frac{1}{N+1}\,\delta p/\Delta C_i, \qquad i = 1, ..., N-1,$$

where

$$\delta p = \Delta p - \left(\bar{p}_\rho\,\Delta\rho + \bar{p}_e\,\Delta e + \sum_{i=1}^{N-1} \bar{p}_{C_i}\Delta C_i\right)$$

is the residual of Eq. (3.17) when we substitute $(\bar{p}_e, \bar{p}_\rho, \bar{p}_{C_i})$ for $(\hat{p}_e, \hat{p}_\rho, \hat{p}_{C_i})$.

Equations (3.22) are simple and easy to implement; however, a potential flaw exists: when Δe, $\Delta\rho$, or ΔC_i vanishes, $\hat{p}_e$, $\hat{p}_\rho$, or $\hat{p}_{C_i}$ becomes indeterminate. In practice, if Δe, $\Delta\rho$, or ΔC_i vanishes, $\hat{p}_e$ simply reduces to $\bar{p}_e$, $\hat{p}_\rho$ to $\bar{p}_\rho$, or $\hat{p}_{C_i}$ to $\bar{p}_{C_i}$.

A better scaling is

$$R = \bar{p}_e, \qquad E = \bar{p}_\rho, \qquad M_i = \bar{p}_{C_i}; \tag{3.23a}$$

we then have $(\alpha, \alpha_1, \alpha_2, \ldots) = (1, 1, 1, \ldots)$, yielding

$$y_s = 1 + \beta\Psi, \tag{3.23b}$$

$$z_{i_s} = 1 + \gamma_i\Psi, \qquad i = 1, ..., N-1,$$

where

$$\Psi = \frac{\Delta p\,\delta p}{(\bar{p}_e\Delta e)^2 + (\bar{p}_\rho\,\Delta\rho)^2 + \sum_{i=1}^{N-1}(\bar{p}_{C_i}\Delta C_i)^2}. \tag{3.23c}$$

Substituting Eq. (3.19c) to Eq. (3.23), we obtain

$$\hat{p}_e = \bar{p}_e\left(1 + \frac{\bar{p}_e\Delta e}{(\bar{p}_e\Delta e)^2 + (\bar{p}_\rho\,\Delta\rho)^2 + \sum_{i=1}^{N-1}(\bar{p}_{C_i}\Delta C_i)^2}\,\delta p\right),$$

$$\hat{p}_\rho = \bar{p}_\rho\left(1 + \frac{\bar{p}_\rho\Delta\rho}{(\bar{p}_e\Delta e)^2 + (\bar{p}_\rho\Delta\rho)^2 + \sum_{i=1}^{N-1}(\bar{p}_{C_i}\Delta C_i)^2}\,\delta p\right), \tag{3.24}$$

$$\hat{p}_{C_i} = \bar{p}_{C_i}\left(1 + \frac{\bar{p}_{C_i}\Delta C_i}{(\bar{p}_e\Delta e)^2 + (\bar{p}_\rho\Delta\rho)^2 + \sum_{i=1}^{N-1}(\bar{p}_{C_i}\Delta C_i)^2}\,\delta p\right), \qquad i = 1, ..., N-1.$$

We may rewrite Eq. (3.24) as

$$\begin{aligned} \hat{p}_e \Delta e &= \bar{p}_e \Delta e + \omega_e \delta p, \\ \hat{p}_\rho \Delta \rho &= \bar{p}_\rho \Delta \rho + \omega_\rho \delta p, \\ \hat{p}_{C_i} \Delta C_i &= \bar{p}_{C_i} \Delta C_i + \omega_{C_i} \delta p, \qquad i = 1, \ldots, N-1, \end{aligned} \tag{3.25a}$$

with

$$\begin{aligned} \omega_e &= \frac{(\bar{p}_e \Delta e)^2}{(\bar{p}_e \Delta e)^2 + (\bar{p}_\rho \Delta \rho)^2 + \sum_{i=1}^{N-1} (\bar{p}_{C_i} \Delta C_i)^2}, \\ \omega_\rho &= \frac{(\bar{p}_\rho \Delta \rho)^2}{(\bar{p}_e \Delta e)^2 + (\bar{p}_\rho \Delta \rho)^2 + \sum_{i=1}^{N-1} (\bar{p}_{C_i} \Delta C_i)^2}, \\ \omega_{C_i} &= \frac{(\bar{p}_{C_i} \Delta C_i)^2}{(\bar{p}_e \Delta e)^2 + (\bar{p}_\rho \Delta \rho)^2 + \sum_{i=1}^{N-1} (\bar{p}_{C_i} \Delta C_i)^2}, \qquad i = 1, \ldots, N-1. \end{aligned} \tag{3.25b}$$

The meaning of Eq. (3.25a) is that the residual δp is distributed over the terms $\hat{p}_e \Delta e$, $\hat{p}_\rho \Delta \rho$, and $\hat{p}_{C_i} \Delta C_i$ in Eq. (3.17) with weights ω_e, ω_ρ, and ω_{C_i}. In the case that Δe, $\Delta \rho$, or ΔC_i vanishes, the corresponding weight vanishes. It is evident from Eq. (3.23) that choosing a different scaling (R, E, M_i) just amounts to choosing different weights for distributing the residual over its constituent terms. The choice of Eq. (3.22), for example, amounts to simply taking $\omega_e = \omega_\rho = \omega_{C_i} = 1/(N+1)$. Another viable choice is

$$\omega_e = \frac{|\bar{p}_e \Delta e|}{|\bar{p}_e \Delta e| + |\bar{p}_\rho \Delta \rho| + \sum_{i=1}^{N-1} |\bar{p}_{C_i} \Delta C_i|}, \tag{3.26}$$

with ω_ρ and ω_{C_i} defined similarly.

All formulas presented above return the standard values $(\hat{p}_e, \hat{p}_\rho, \hat{p}_{C_i}) = (\bar{p}_e, \bar{p}_\rho, \bar{p}_{C_i})$ for a calorically perfect gas, since in this case Q lies on the surface D and the pressure residual δp vanishes.

4. Chemistry Model

The present finite-rate chemistry model includes five species (O_2, N_2, O, N, NO) and eleven elementary reaction steps for the dissociation and recombination of air. The kinetics data for this model are taken from Dunn and Kang [17], except that the ions and free electron, and the associated reaction steps are not included. The reactions and the rate coefficients are given in Table I. The neglect of the effect of ionization is solely for the sake of simplicity (the complete model with ionization reactions involves 11 species and 26 elementary reaction steps); there is no fundamental difficulty in generalizing the present formulation to an ionizing gas.

TABLE I

Chemical Reactions and Rate Coefficients Used in Nonequilibrium Calculations

NO.	REACTION	FORWARD RATE COEFF, k_F	BACKWARD RATE COEFF, k_B	THIRD BODY, M
	FORWARD DIRECTION	$cm^3/mole\ sec$	$cm^3/mole\ sec$ OR $cm^6/mole^2\ sec$	——
1	$O_2 + M \rightarrow 2O + M$	$3.6 \times 10^{18} T^{-1.0} \exp(-5.95 \times 10^4/T)$	$3.0 \times 10^{15} T^{-0.5}$	N, NO
2	$N_2 + M \rightarrow 2N + M$	$1.9 \times 10^{17} T^{-0.5} \exp(-1.13 \times 10^5/T)$	$1.1 \times 10^{16} T^{-0.5}$	O, NO, O_2
3	$NO + M \rightarrow N + O + M$	$3.9 \times 10^{20} T^{-1.5} \exp(-7.55 \times 10^4/T)$	$1.0 \times 10^{20} T^{-1.5}$	O_2, N_2
4	$O + NO \rightarrow N + O_2$	$3.2 \times 10^9 T^1 \exp(-1.97 \times 10^4/T)$	$1.3 \times 10^{10} T^{1.0} \exp(-3.58 \times 10^3/T)$	
5	$O + N_2 \rightarrow N + NO$	$7.0 \times 10^{13} \exp(-3.8 \times 10^4/T)$	1.56×10^{13}	
6	$N + N_2 \rightarrow N + N + N$	$4.085 \times 10^{22} T^{-1.5} \exp(-1.13 \times 10^5/T)$	$2.27 \times 10^{21} T^{-1.5}$	
7	$O_2 + O \rightarrow 2O + O$	$9.0 \times 10^{19} T^{-1.0} \exp(-5.95 \times 10^4/T)$	$7.5 \times 10^{16} T^{-0.5}$	
8	$O_2 + O_2 \rightarrow 2O + O_2$	$3.24 \times 10^{19} T^{-1.0} \exp(-5.95 \times 10^4/T)$	$2.7 \times 10^{16} T^{-0.5}$	
9	$O_2 + N_2 \rightarrow 2O + N_2$	$7.2 \times 10^{18} T^{-1.0} \exp(-5.95 \times 10^4/T)$	$6.0 \times 10^{15} T^{-0.5}$	
10	$N_2 + N_2 \rightarrow 2N + N_2$	$4.7 \times 10^{17} T^{-0.5} \exp(-1.13 \times 10^5/T)$	$2.72 \times 10^{16} T^{-0.5}$	
11	$NO + M \rightarrow N + O + M$	$7.8 \times 10^{20} T^{-1.5} \exp(-7.55 \times 10^4/T)$	$2.0 \times 10^{20} T^{-1.5}$	O, N, NO

For a set of N_R elementary reactions involving N species, the rate equations can be written in the general form

$$\sum_{j=1}^{N} \nu'_{ij} n_j \underset{k_{b_i}}{\overset{k_{f_i}}{\rightleftharpoons}} \sum_{j=1}^{N} \nu''_{ij} n_j, \qquad i = 1, 2, ..., N_R, \tag{4.1}$$

where ν'_{ij} and ν''_{ij} are the stoichiometric coefficients for species j appearing as a reactant in the ith forward and backward reactions, respectively, and n_j is the molar concentration for species j ($n_j = C_j/W_j$). Also, k_{f_i} and k_{b_i} respectively are the forward and backward reaction rate constants for the ith reaction step. The reaction rate constant k_i (k_{f_i} or k_{b_i}) is given empirically by the Arrhenius expression,

$$k_i = A_i T^{m_i} e^{-E_i/R_u T}, \tag{4.2}$$

where E_i represents the activation energy and A_i and m_i are constants.

From (4.1), the rate of change of molar concentration of species j by reaction step i is

$$(\dot{n}_j)_i = (\nu''_{ij} - \nu'_{ij}) \left(k_{f_i} \prod_{l=1}^{N} n_l^{\nu'_{il}} - k_{b_i} \prod_{l=1}^{N} n_l^{\nu''_{il}} \right). \tag{4.3}$$

The total rate of change of molar concentration of species j is

$$\dot{n}_j = \sum_{i=1}^{N_R} (\dot{n}_j)_i, \tag{4.4}$$

from which follows the rate of change of mass concentration for species j,

$$S_j = W_j \dot{n}_j, \tag{4.5}$$

which appears in (3.1).

We observe that the chemical source term S_j depends exponentially on temperature. We also observe that, although pressure does not appear explicitly in the source expression, S_j is a strong function of pressure due to the influence of pressure on density and species concentrations.

It should also be noted that, because of the vastly different chemical time scales, that may be involved in the elementary reactions, and the exponential dependence of the source terms on temperature, the set of species equations in (3.1) may become very stiff over certain temperature ranges.

To mitigate the stiffness problem, chemical source terms appearing in (3.1) are treated in an implicit fashion; in this way the convergence rate (for steady nozzle problem) or the numerical stability is not appreciably degraded. For maximum stability in steady-state calculations the source terms are nominally evaluated at the end of the time step (backward-Euler scheme); actually, the nonlinear implicit equations are linearized about the initial state. This procedure is only first-order

accurate in time; for unsteady calculations second-order accuracy is preferable. This can be achieved by integrating the source term in time with the trapezoidal rule (Crank–Nicholson), using the linearized equations to iteratively solve the nonlinear equations. The source-term Jacobian, $\mathbf{H} = \partial \mathbf{S}/\partial \mathbf{U}$, resulted from the linearization procedure, has the following general form:

$$\mathbf{H} = \begin{bmatrix} 0 & 0 & 0 & 0 & 0 & 0 & 0 \\ 0 & 0 & 0 & 0 & 0 & 0 & 0 \\ 0 & 0 & 0 & 0 & 0 & 0 & 0 \\ \dfrac{\partial S_1}{\partial \rho} & \dfrac{\partial S_1}{\partial (\rho u)} & \dfrac{\partial S_1}{\partial (\rho E)} & \dfrac{\partial S_1}{\partial C_1} & \dfrac{\partial S_1}{\partial C_2} & \dfrac{\partial S_1}{SC_3} & \dfrac{\partial S_1}{\partial C_4} \\ \dfrac{\partial S_2}{\partial \rho} & \dfrac{\partial S_2}{\partial (\rho u)} & \dfrac{\partial S_2}{\partial (\rho E)} & \dfrac{\partial S_2}{\partial C_1} & \dfrac{\partial S_2}{\partial C_2} & \dfrac{\partial S_2}{\partial C_3} & \dfrac{\partial S_2}{\partial C_4} \\ \dfrac{\partial S_3}{\partial \rho} & \dfrac{\partial S_3}{\partial (\rho u)} & \dfrac{\partial S_3}{\partial (\rho E)} & \dfrac{\partial S_3}{\partial C_1} & \dfrac{\partial S_3}{\partial C_2} & \dfrac{\partial S_3}{\partial C_3} & \dfrac{\partial S_3}{\partial C_4} \\ \dfrac{\partial S_4}{\partial \rho} & \dfrac{\partial S_4}{\partial (\rho u)} & \dfrac{\partial S_4}{\partial (\rho E)} & \dfrac{\partial S_4}{\partial C_1} & \dfrac{\partial S_4}{\partial C_2} & \dfrac{\partial S_4}{\partial C_3} & \dfrac{\partial S_4}{\partial C_4} \end{bmatrix}. \tag{4.6}$$

Noting that for a given chemical kinetics model the source term is a function of only temperature and species concentration, i.e., $S_j = S_j(T, C_i, i = 1, ..., N)$, as is the specific internal energy $e = e(T, C_i/\rho, i = 1, ..., N)$, the elements in the Jacobian matrix, (4.6), can be evaluated via the chain-rule, e.g.,

$$\begin{aligned} \left.\frac{\partial S_j}{\partial \rho}\right|_{\rho u, \rho_E, C_{i,i=1,N-1}} &= \left.\frac{\partial S_j}{\partial T}\right|_{C_{i,i=1,N-1}} \left.\frac{\partial T}{\partial e}\right|_{\rho, C_{i,i=1,N-1}} \left.\frac{\partial e}{\partial \rho}\right|_{\rho u, \rho_E, C_{i,i=1,N-1}} \\ &= \frac{1}{\rho C_v}(u^2 - E) \left.\frac{\partial S_j}{\partial T}\right|_{C_{i,i=1,N-1}}; \end{aligned} \tag{4.7}$$

here

$$\begin{aligned} \left.\frac{\partial S_j}{\partial T}\right|_{C_{i,i=1,N-1}} = W_j \sum_{i=1}^{N_R} \left((v''_{ij} - v'_{ij}) \left[\frac{k_{f_i}}{T} \left(m_{f_i} + \frac{E_{f_i}}{R_u T} \right) \prod_{l=1}^{N} n_l^{v'_{il}} \right.\right. \\ \left.\left. - \frac{k_{b_i}}{T} \left(m_{b_i} + \frac{E_{b_i}}{R_u T} \right) \prod_{l=1}^{N} n_l^{v''_{il}} \right] \right). \end{aligned} \tag{4.8}$$

Similarly,

$$\begin{aligned} \left.\frac{\partial S_j}{\partial (\rho u)}\right|_{\rho, \rho_E, C_{i,i=1,N-1}} &= \left.\frac{\partial S_j}{\partial T}\right|_{C_{i,i=1,N-1}} \left.\frac{\partial T}{\partial e}\right|_{\rho, C_{i,i=1,N-1}} \left.\frac{\partial e}{\partial (\rho u)}\right|_{\rho, \rho_E, C_{i,i=1,N-1}} \\ &= -\frac{u}{\rho C_v} \left.\frac{\partial S_j}{\partial T}\right|_{C_{i,i=1,N-1}}, \end{aligned} \tag{4.9}$$

$$\left.\frac{\partial S_j}{\partial(\rho E)}\right|_{\rho,\rho_u,C_{i,i=1,N-1}} = \left.\frac{\partial S_j}{\partial T}\right|_{C_{i,i=1,N-1}} \left.\frac{\partial T}{\partial e}\right|_{\rho,C_{i,i=1,N-1}} \left.\frac{\partial e}{\partial(\rho E)}\right|_{\rho,\rho_u,C_{i,i=1,N-1}}$$

$$= \frac{1}{\rho C_v} \left.\frac{\partial S_j}{\partial T}\right|_{C_{i,i=1,N-1}}, \tag{4.10}$$

$$\left.\frac{\partial S_j}{\partial C_i}\right|_{\rho,\rho_u,\rho_E,C_{l,l=1,N-1,l\neq i}} = \left.\frac{\partial S_j}{\partial C_i}\right|_T + \left.\frac{\partial S_j}{\partial T}\right|_{C_{i,i=1,N-1}} \left.\frac{\partial T}{\partial C_i}\right|_{\rho,\rho u,\rho_E,C_{l,l=1,N-1,l\neq i}}$$

$$= W_j \sum_{k=1}^{N_R} \left[(v''_{ij} - v'_{ij}) \left(\frac{v'_{ki}}{C_i} k_{fi} \prod_{l=1}^{N} n_l^{v'_{kl}} \right.\right.$$

$$\left.\left. - \frac{v''_{ki}}{C_i} k_{bi} \prod_{l=1}^{N} n_l^{v''_{kl}} \right) \right] - \frac{(e_i - e_N)}{\rho C_v} \left.\frac{\partial S_j}{\partial T}\right|_{C_{i,i=1,N-1}}. \tag{4.11}$$

We note that, despite the implicit treatment of chemical source terms, the set of species equations still becomes very difficult to solve numerically at regions where temperature is very high and chemical reactions are intensive. In this case, the chemical time scales tend to be many orders of magnitude smaller than the flow time scales or the time steps required for a cost-effective solution. To completely overcome this difficulty, exceedingly small time steps have to be adopted in the numerical calculations. Since it is not our interest in this study to investigate the high temperature chemical kinetics, we have not chosen to use CFL numbers which are small enough to resolve the chemical time scales. The consequence of using large numerical time steps (as compared to chemical times) is that numerical fluxtuations appear in the species concentration predictions in some regions of the flows, as will be seen in the Numerical Test Section.

5. Numerical Test

Numerical tests have been conducted to validate the accuracy of the present formulation. Some extreme cases of one-dimensional unsteady shock-tube and steady nozzle problems are presented in this paper. The performance of these split fluxes for finite-rate chemistry analysis is compared against the equilibrium results of [10].

The Euler equations are integrated using the explicit Lax–Wendroff scheme. To obtain a crisp and monotone shock representation, a TVD scheme based on the above split formulas, as described in [10], is employed, along with the super-Bee limiter [18] for steepening of the contact discontinuity. The present scheme is second-order accurate both in space and time.

For all the test cases to be discussed in the following, initial conditions or inflow conditions are assumed to be air at equilibrium state.

5.1. *Shock-Tube Problem*

The initial conditions are those used in [5, 10]:

for $0 \leqslant x \leqslant 0.5$ cm,

$$p_4 = 100 \text{ atm},$$
$$T_4 = 9000 \text{ K},$$
$$u_4 = 0;$$

for $0.5 \leqslant x \leqslant 1$ cm,

$$p_1 = 1 \text{ atm},$$
$$T_1 = 300 \text{ K},$$
$$u_1 = 0.$$

Figures 1–3 show the numerical results of the Roe, Van Leer, and Steger–Warming splittings for, respectively, ρ/ρ_4, u/a_4, p/p_4, and e/e_4, for both the chemical equilibrium and nonequilibrium cases. This is a difficult case to calculate, as the initial jumps in temperature and pressure across the contact are large, about

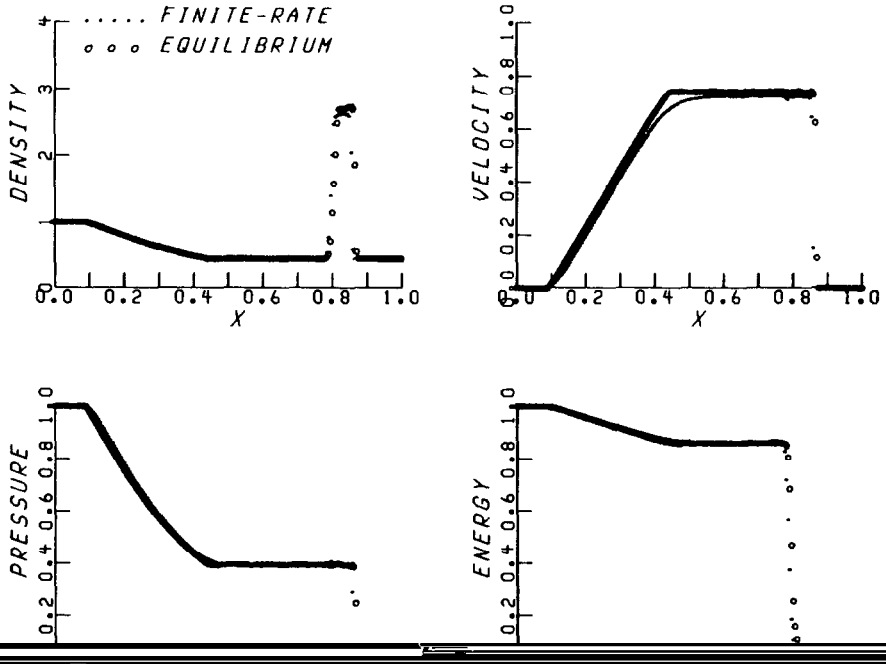

FIG. 1. Shock-tube problem, Roe flux-difference splitting.

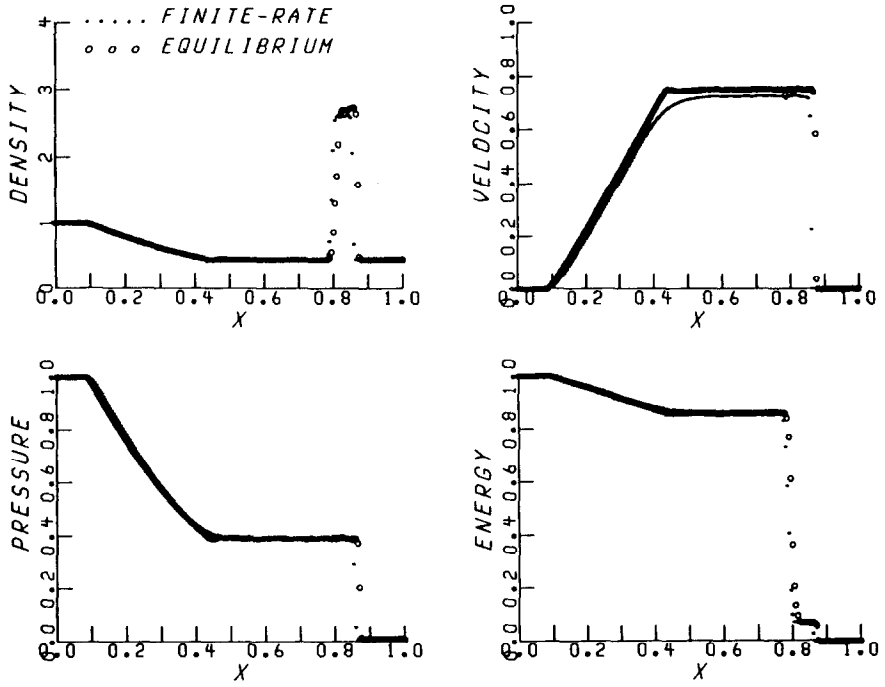

FIG. 2. Shock-tube problem, van Leer flux-vector splitting.

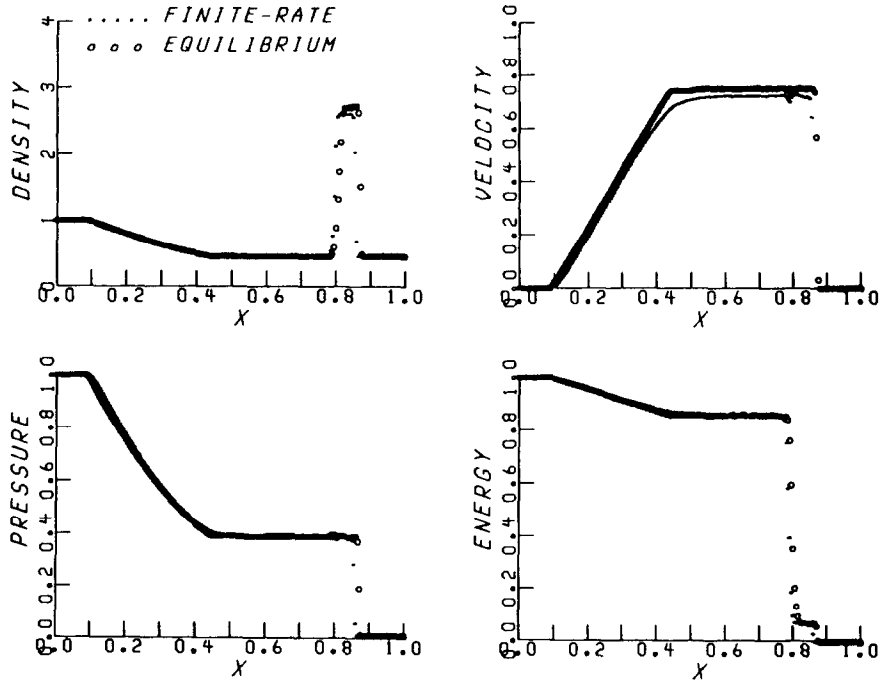

FIG. 3. Shock-tube problem, Steger–Warming flux-vector splitting.

one to two orders of magnitude, and consequently the compositions are completely different. It has been our experience [8, 9] that the TVD flux-splitting scheme can handle large differences in pressure very well, but not as well if there are also large differences in temperature. Nevertheless, our numerical results generally show very crisp profiles of shock and contact discontinuities. Among all the three splittings, the Roe scheme gives the best results, especially near the contact discontinuity. Because of the finite relaxation time, the nonequilibrium case shows a weaker jump in density across the contact and a smoother variation in velocity around the tail of the expansion fan.

The temperature and species molar fractions obtained using the Roe splitting are shown in Fig. 4. The sharp peak in the equilibrium NO molar fraction is a numerical result produced by the smearing of internal energy at the contact discontinuity [10]. This is because the NO molar fraction is a very strong, non-monotone function of temperature (internal energy) and is most stable at some intermediate temperature across the "numerical" contact discontinuity. On the other hand, the oscillations in O and NO molar fractions across the contact discontinuity in the finite-rate case are the results of numerical inaccuracy caused by the exceedingly large chemical source terms and small chemical time scales in the species equations. It is noted that the spurious fluctuations of the molar fractions in the finite-rate

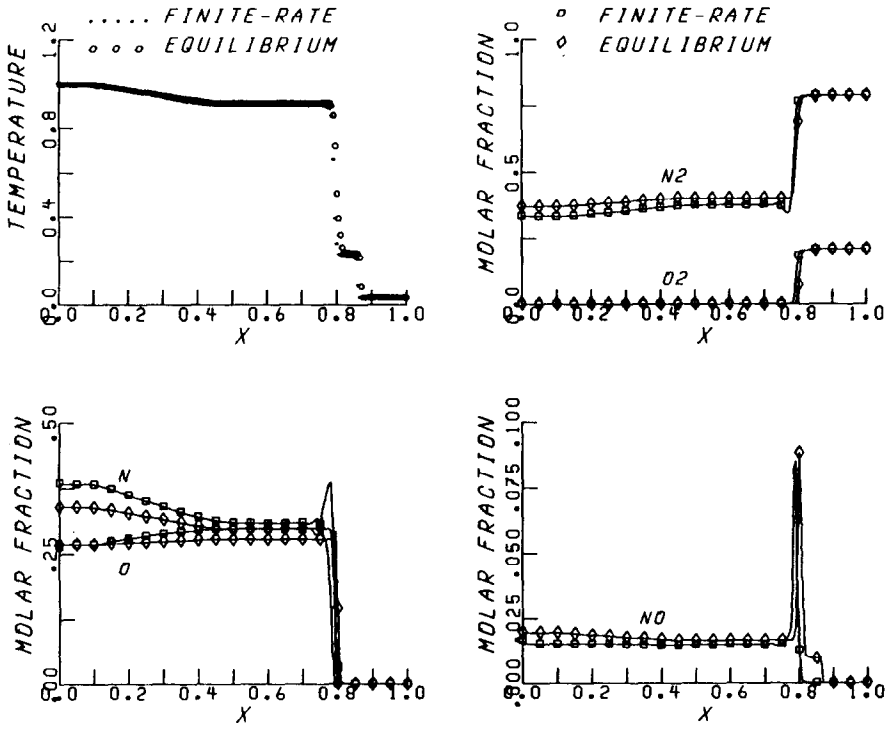

FIG. 4. Shock-tube problem, temperature and species molar fractions.

predictions can be removed by using smaller time steps in the calculations; a CFL number smaller than 10^{-2} is required to remove most of the fluctuations for the shock-tube case considered here. The results shown in Figs. 1–4 are obtained using CFL of 0.5.

5.2. *Steady Nozzle-Flow Problem*

Calculated results using Roe splitting for the steady flow with a shock in a 1D divergent nozzle are given in Figs. 5–6. Figure 5 shows the results for ρ/ρ_∞, u/a_∞, p/p_∞, and e/e_∞. The nozzle area ratio is 10 and the inflow conditions are for equilibrium air at $T_\infty = 6000$ K and $p_\infty = 10$ atm. Excellent results are obtained by the Roe scheme with a monotone and sharp shock structure. Figure 6 illustrates the temperature (T/T_∞) and species molar fraction predictions. Because of the rapid decrease in flow temperature and pressure through the nozzle throat, the chemical reactions are slowed down to the point that finite-rate effects become significant. Consequently, noticeable differences are observed in the predictions of temperature and concentrations of the air dissociation products O, NO, and N, between the equilibrium and nonequilibrium approaches. Calculations using the Steger–Warming and Van Leer schemes were also conducted for the same flow conditions. The results obtained with these two schemes are almost exactly the same as those of the Roe scheme, and therefore they are not shown here.

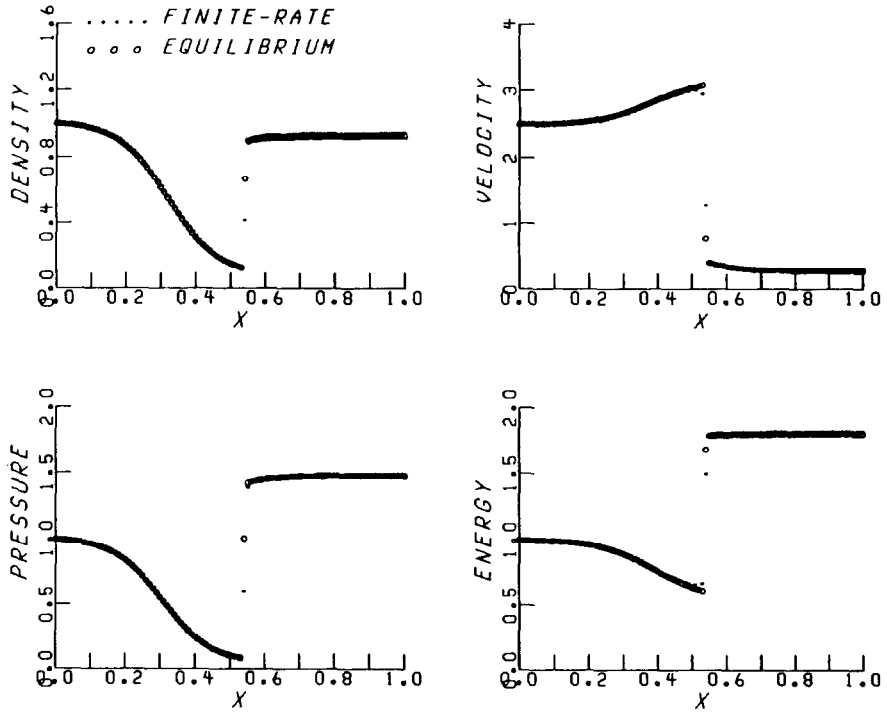

FIG. 5. Divergent-nozzle problem, Roe flux-difference splitting, nozzle area ratio = 10.

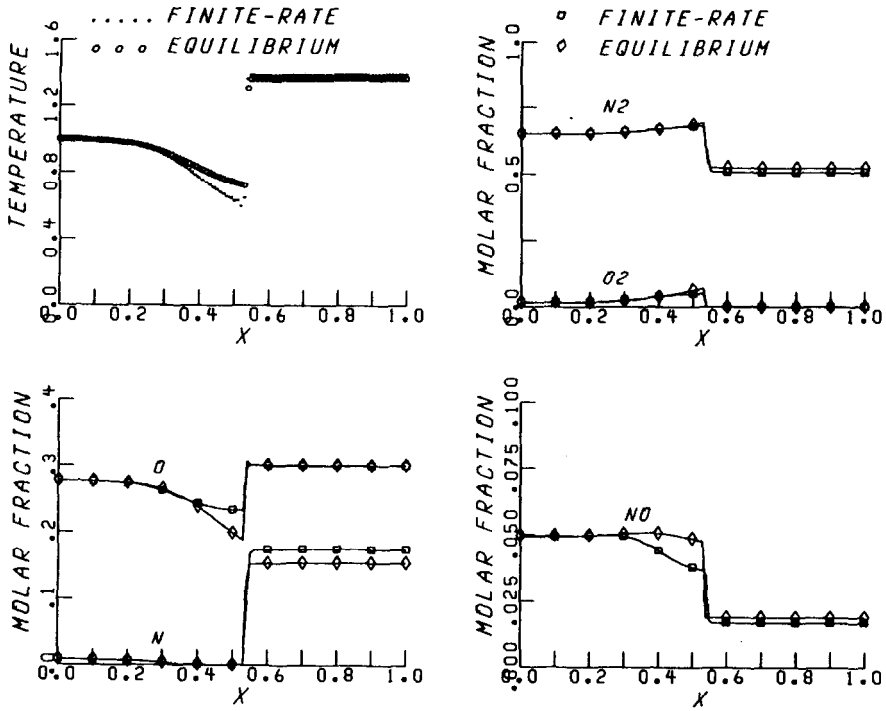

FIG. 6. Divergent-nozzle problem, temperature and species molar fractions.

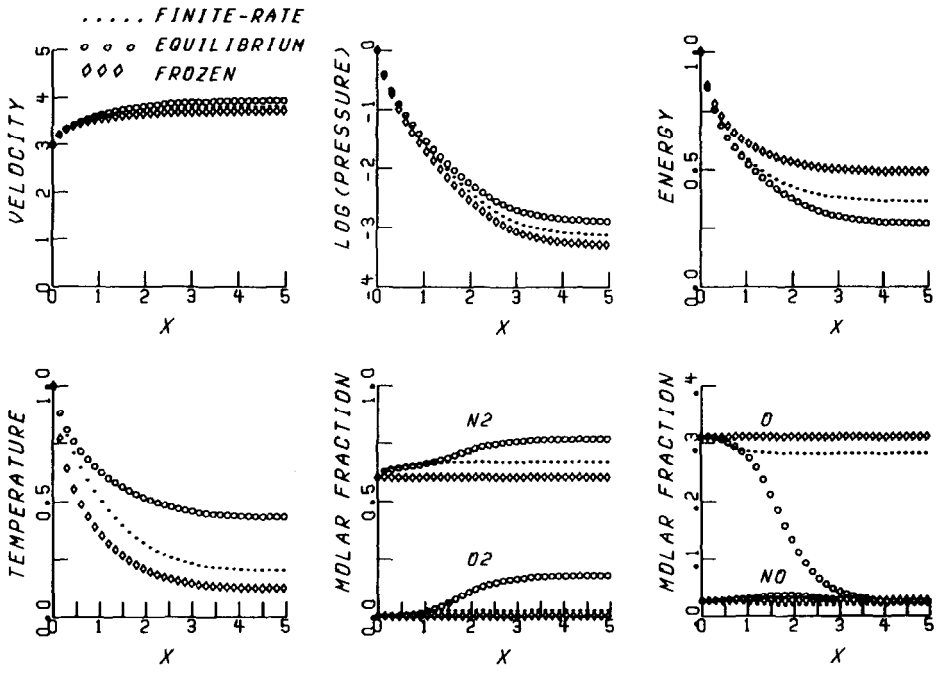

FIG. 7. Divergent-nozzle problem, Roe flux-difference splitting, nozzle area ratio = 200.

To further illustrate the nonequilibrium effect, results for air flow, with the same inlet conditions as the previous case, expanding through a divergent nozzle of area ratio 200 are presented in Fig. 7. Because of the high temperature and pressure involved, initially the finite-rate results coincide with equilibrium calculations almost exactly. But, because of the very large area ratio of the nozzle, the temperature and pressure rapidly decrease to the values at which the flow is essentially chemically frozen, as clearly depicted in the molar fraction plots. This equilibrium-sudden freezing behavior of the hypersonic nozzle flow was also discussed by Bray [19].

Concluding Remarks

Formulations of inviscid flux splitting algorithms for chemical nonequilibrium gases are described. Special care has been exercised to avoid unnecessary assumptions, approximations, or auxiliary quantities. The calculated results demonstrate the validity as well as the advantage of the present approach. The numerical results also indicate that improvement is needed for better handling the large disparity in chemical and flow scales at high temperatures.

References

1. J. L. Steger and R. F. Warming, *J. Comput. Phys.* **40**, 263 (1981),
2. B. van Leer, Flux-vector spitting for the Euler equations, in *Lecture Notes in Physics*, Vol. 170 (Springer-Verlag, New York/Berlin, 1982), p. 507.
3. P. L. Roe, *J. Comput. Phys.* **43**, 357 (1981).
4. P. Collela and H. M. Glaz, *J. Comput. Phys.* **59**, 264 (1985).
5. B. Grossman and R. W. Walters, AIAA Paper 87–1117–CP, 1987 (unpublished).
6. M. Vinokur and Y. Liu, AIAA Paper 88–0127, 1988 (unpublished).
7. M. Vinokur NASA CR-177512, 1988 (unpublished).
8. M. Vinokur and J.-L. Montagne, NASA CR-177513, 1988 (unpublished).
9. P. Glaister, *J. Comput. Phys.* **74**, 382 (1988).
10. M.-S. Liou, B. van Leer, and J.-S. Shuen, *J. Comput. Phys.* **87**, 1 (1990).
11. B. Grossman and P. Cinnella, ICAM Report 88–08–03, Virginia Polytechnic Institute and State University, 1988 (unpublished).
12. R. Abgrall, private communication, 1989.
13. B. Grossman, P. Cinnella, and J. Garrett, AIAA Paper 89–1653, 1989 (unpublished).
14. M.-S. Liou, AIAA Paper 87–0355, 1987 (unpublished).
15. B. J. Mcbride, private communication, 1988.
16. B. Stoufflet, private communication, 1988.
17. M. G. Dunn and S. W. Kang, NASA CR–2232, 1973 (unpublished).
18. P. L. Roe, *Annu. Rev. Fluid Mech.* **18**, 337 (1986).
19. K. N. C. Bray, *Nonequilibrium Flows*, edited by P. P. Wegener (Dekker, New York, 1970), p. 93.